Frequency Domain Estimation Method of The Characteristic Period of The P Wave of Earthquakes

Codrin Donciu , Elena Serea * , Marinel Costel Temneanu

Posted Date: 3 November 2023

doi: 10.20944/preprints202311.0203.v1

Keywords: earthquake; P wave; characteristic period; frequency domain.

Article

Frequency Domain Estimation Method of the Characteristic Period of the P Wave of Earthquakes

Codrin Donciu, Elena Serea * and Marinel Costel Temneanu

Faculty of Electrical Engineering, "Gheorghe Asachi" Technical University of Iași, 700050 Iași, Romania
* Correspondence: edanila@tuiasi.ro; Tel.: 0040740481758

Abstract: The earthquake alert of the early warning systems is based on the delay that the S waves have in reference to the P waves and on the interpretation of the P waves' specific parameters. One of the most used parameters for estimating the moment magnitude of an earthquake is the characteristic period measured in the first 3 seconds of the appearance of the P wave. The typical method determines the characteristic period in the time domain, based on the velocity wave and the displacement wave. In the present work, we present a method for estimating the frequency of the characteristic period. This method includes zero padding of the P wave sequence, conversion of the extended sequence from the time domain to the frequency domain, the identification of local frequency maxima and the calculation of the weighted average of the frequency based on the identified maxima. Tests conducted on synthetic signals, as well as standard deviation evaluation tests for simultaneous recordings on several stations, reveal better performance to the usual method.

Keywords: earthquake; P wave; characteristic period; frequency domain

1. Introduction

An earthquake occurs when a fault in the Earth's crust slips, a phenomenon that arise very often. Large earthquakes emerge similarly as small earthquakes, but continue to grow as long as the force applied to the fault is greater than its resistance. Each one-unit increase in magnitude is associated with a rupture approximately 5 times longer (for example, a 5Mw earthquake is caused by a slip on a fault about 2 kilometers long, while a 6Mw earthquake is caused by a slip on a fault about 10 kilometers long).

Earthquakes repeatedly rupture a given part of a fault, hence the concept of a seismic cycle. This basic cycle should not be interpreted as a typical recurrence of time, but as a slipping behavior, where time scale ranges from regular earthquakes to slow slips events. It is acknowledged that a seismic cycle comprises six main stages: (1) Over years, small and medium active faults with increased friction break continuously, resulting in a uniform rate of seismicity. (2) Asperities on the fault surface become locked, resulting in stress accumulation and decreasing seismic activity. (3) Days before the largest earthquake in a sequence (main-shock), important asperities progressively break along some sections (the foreshock stage). (4) Over a scale of hours, accumulated stresses overcome friction and blockages in the main asperities, causing the largest magnitude earthquake of the cycle. (5) Stress relaxation occurs and many aftershocks of smaller magnitude are generated over several weeks or months; this stops when new asperities become locked. (6) Lastly, the system returns to the initial, long-term, state [1]. Following the seismic cycle, where six energy transition phases are succeeding, results that the occurrence of an earthquake can be assessed using entropy. The first three phases (inter-seismic period) are characterized by low entropy and the last two phases (post-seismic period) are characterized by progressively decreasing entropy, returning to the initial state. The highest entropy value is found during the main-shock, in phase 4, as the rupture process triggers earthquakes with magnitudes of all sizes in a disordered way. The seismic studies are founded on various meanings of the entropy concept, depending on the scientific perspective: in statistical physics, entropy is related to the numbers of microscopic configurations of a thermodynamic system, specified by macroscopic variables. In statistical mechanics, entropy, observed as a macroscopic disorder, is a measure of the number of microstates in which a system can be arranged (the higher

 doi:10.20944/preprints202311.0203.v1

the number of microstates, the higher the entropy [2]). In information science, entropy is defined as the sheer amount of information needed to specify the full set of microstates of the system [3]. However, entropy is used along with other physical quantities to describe quantitatively the chaotic and non-linear behavior of earthquakes, of any size and in any environment [4]. Pursuant to the premise of seismic cycles, stress builds up for an extended period over a large portion of a fault and then is released suddenly in a large earthquake [5], so the probability of a particular portion of a fault rupturing twice in quick succession should be low and large earthquakes might be quasi periodic [6].

The intense ground motions caused by an earthquake pose a major hazard to the population living in the vicinity of the epicenter and can cause substantial damage to roads, buildings and other infrastructures. Among natural disasters, earthquakes account for about a fifth of economic losses and are responsible for an average of about 20,000 deaths per year.

At the moment it is impossible to accurately foresee the moment or the place of a destructive earthquake occurrence. Estimation for anticipating near the event can be computed with early warning systems (EEW - Earthquake Early Warning). If the rupture expansion process of a large earthquake is predictable and if it produces observable signatures different from that of smaller events are fundamental questions related to the potential for earthquake early warning and probabilistic forecasting [7]. The densification and technological evolution of seismic monitoring networks, as well as the exponential growth of computing resources, provide the opportunity to explore seismic sources at new time and frequency scales, significantly improving the level of detection. Despite the noticeable advances of early warning systems, they must be refined from the point of view of maximizing the warning time and minimizing the number of false alarms [8].

Beside the moment and location, the predictability of an earthquake size is equally important. To determine how different the earthquake rupture and radiated seismic waves of different-sized earthquakes are, is a classic issue in seismology [7]. The initial waveforms of large earthquakes are complex, but the very beginnings can be similar to those of small events. There was confirmed in [9, 10] that closely located earthquakes share quite similar initial waveforms, despite their magnitude, most waveforms being indistinguishable during the first 0.07 s. This evidence appoints that, from a practical perspective, the onset of a seismic waveform is not a sufficient input for the efficient operation of the EEW systems, for any size and location of earthquakes, and that there is a need to include in detection algorithm design for specific estimation methods. EEW systems can trigger anticipative alarms because the onset of the earthquake is achieved by non-destructive primary P waves and continues with destructive secondary S waves. Since P waves have a higher travel speed, they will reach their destination first and can be a source of information regarding the destructive waves that will reach their destination later. Although the speed of movement of P and S waves (elastic waves) varies depending on the composition of the soil, the ratio between the two speeds remains relatively constant, with P waves moving approximately 1.7 times faster than S waves. The earthquake warning of EEW systems is based on the delay that S waves have related to P waves. This delay increases with the distance from the epicenter of the earthquake. For example, at 200 km from the epicenter, the S wave arrives about 20 seconds behind the P wave. The warning based on the P wave is used to allow the movement of people to the safety point of the building, or for the automatic activation of some control devices (stopping the gas supply, stopping the electricity supply, unlocking access doors, slowing down the speed of trains, etc.). The relatively short time between the warning (P wave) and the destructive start of the earthquake (S wave) does not allow occupants leaving the building. All inhabitants should have established in advance, a maximum safety place inside to take shelter in case of an earthquake.

The concept of EEW was first introduced by J.D. Cooper in 1868 [11], proposing the installation of seismic sensors that would transmit an electrical signal when an earthquake occurs, but the practical implementation was achieved barely in 1960, within a high-speed train derailment avoidance system in Japan [12].

After several decades of development, EEW systems are currently operational and provide alerts to population (Japan, Taiwan, Mexico, South Korea), institutions or limited users (India, Romania,

Preprints (www.preprints.org) | NOT PEER-REVIEWED | Posted: 3 November 2023 doi:10.20944/preprints202311.0203.v1

Turkey, and the West Coast of the United States), or are under development or testing (Italy, Chile, Costa Rica, EI Salvador, Nicaragua, Switzerland, Israel, Beijing and the Fujian region of China) [13].

Within an EEW system, the following sequences may exist between the occurrence of an earthquake and the triggering of an alarm [14]:

- earthquake detection, based on the STA/LTA ratio (Short Term Average / Long Term Average);
- estimating the distance to the place of earthquake's occurrence, based on the difference between the arrival time of the P wave and the arrival time of the S wave, knowing the propagation speed ratio;
- estimation of the Mw magnitude, based on specific parameters of the P wave;
- estimating the intensity of the earthquake for a place of interest (target site), or PGA (Peak Ground Acceleration);
- alarm decision.

The core of the algorithm is the estimation of the earthquake's magnitude. The assessment is made using the displacement waveform and must contain as much of the low frequency component of the frequency spectrum as possible to avoid magnitude saturation [15].

Among the first P wave parameters used for magnitude estimation is the predominant period defined as the period corresponding to the maximum amplitude in the frequency spectrum of the displacement [16, 17]. An approach to the predominant period, based on the velocity wave, is presented in [18] and is known as the τp method. Since this method contained numerous limitations related to the sampling frequency and the signal processing, an improved version was proposed in [19], where the predominant period is continuously calculated and its maximum value (τp max) is to be determined. Another magnitude estimation parameter is the characteristic period τc. It refers to both the velocity wave and the displacement wave, being much more stable than τp max [20]. In current studies, the characteristic period is the most ordinarily used parameter for magnitude estimation with regard to the Pd (peak of the displacement wave) [21, 22] or alongside other geophysical parameters, as input data of neural networks [23, 24].

EEW systems are not proper accurately; there is the possibility of providing results that can lead to false alarms. Choosing a small alarm threshold (estimated Mw) can trigger the alarm even though the earthquakes are small, and choosing a large alarm threshold can omit triggering an alarm in case of a large earthquake [25].

2. Methods

To define the characteristic period, were used the ground displacement wave (vertical component) $u(t)$ and the velocity $\dot{u}(t)$, for which the ratio r, defined as follows, was calculated:

$$r = \frac{\int_0^{t_0} \dot{u}^2(t)dt}{\int_0^{t_0} u^2(t)dt} \quad (1)$$

where the integration is over the time interval (0, t_0) after the onset of the P wave. Typically, t_0 is set to 3 seconds. Using Parseval's theorem, according to which states that the energy of an aperiodic signal or the power of a periodic signal in the time domain is equal to the energy or power in the frequency domain, there results:

$$r = \frac{4\pi^2 \int_0^{\infty} f^2 |\hat{u}(f)|^2 df}{\int_0^{\infty} |\hat{u}(f)|^2 df} = 4\pi^2 \langle f^2 \rangle \quad (2)$$

where f is the frequency, $\hat{u}(f)$ is the frequency spectrum of the displacement wave $u(t)$, and $\langle f^2 \rangle$ is the average of f^2 weighted by $|\hat{u}(f)|^2$

The period being the inverse of the frequency, it can be written as the characteristic period to be:

$$\tau_c = \frac{1}{\sqrt{f^2}} = \frac{2\pi}{\sqrt{r}} \quad (3)$$

Preprints (www.preprints.org) | NOT PEER-REVIEWED | Posted: 3 November 2023 doi:10.20944/preprints202311.0203.v1

Although the characteristic period of the P wave is calculated based on the ratio *r*, as can be seen in (3), the characteristic period can also be expressed based on the frequency spectrum of the displacement. More precisely, the squared characteristic frequency is the average of the squared frequencies weighted by the square of the amplitudes in the frequency spectrum:

$$fc^2 = \frac{A_1^2 \cdot f_1^2 + A_2^2 \cdot f_2^2 + \cdots + A_n^2 \cdot f_n^2}{A_1^2 + A_2^2 + \cdots + A_n^2} \quad (4)$$

where $A_1 \ldots A_n$ are the amplitudes of the spectral components, and $f_1 \ldots f_n$ are the frequencies of the spectral components. These values of the spectral components are obtained by applying FFT (Fast Fourier Transform) to the displacement sequence in the time domain (FFT is a common tool used to differentiate seismic signals from ambient ones or those produced by explosions, because the generated spectra can be thus distinguished). At some point, the FFT analysis technique can lead to pitfalls like:

- Sampling may lead to the appearance of the aliasing effect (refers to an effect that causes different signals to become indistinguishable or doubles of each other because a sample rate below the Nyquist rate for a particular signal or too high frequencies present in the signal for a particular sample rate);
- Limiting the acquisition time may cause signal losses or spectral leakage;
- The discrete frequencies in the calculated spectrum may determine the resolution bias error, or "picket fence effect" [26] (when frequency information is only accurate at specific intervals (bins), centered between sample locations).

To remove the errors introduced by the picket fence effect, two methods are available: zero padding [27] and FFT interpolation (IpFFT) [28]. For the presented method, zero padding is the solution used to reduce the distance between bins in frequency, by increasing the sequence of the investigated signal by adding zeros to its end, before the FFT is applied. The extension of the seismic signal with null samples will not negatively influence the application of the method because it is only desired to obtain a specific length of the signal, the studies proving that this is a viable alternative method that improves the readability of the signal frequency [29, 30]. The increased length of the signal has the consequence of decreasing the width between consecutive spectral lines, thus a finer frequency resolution.

Structurally, as can be seen in Figure 1, the method of calculating the characteristic period in the frequency spectrum includes the following steps: from the earthquake displacement waveform (a), are extracted the first 3 seconds of the signal (b), the retrieved sequence is padded with zeros (c) and FFT is applied in order to obtain the frequency spectrum (d). At the level of the frequency spectrum, the local maxima (e) are identified, through which the weighted average of the characteristic frequency is calculated (eq. 4), and implicitly its inverse.

In order to test the proposed method, a comparative study was carried out between the classic method, from the time domain that uses the ratio between speed and displacement (M1), the method from the frequency domain based on eq.4 for calculating the characteristic frequency (M2) and the proposed method (M3). The test signals on the basis of which the characteristic frequency and the characteristic period were calculated, are signals synthesized by summing sinusoidal signals with imposed frequencies and amplitudes. The reference frequency, against which the absolute error was calculated, was obtained using the signal synthesis values (the amplitudes and frequencies of the sinusoidal signals summed to obtain the test signals). The framework of signals acquisition is similar to the physical one used in the acquisition of the seismic signals: sampling frequency 200 Hz, acquisition time 3 seconds, total number of acquired points 600.

Preprints (www.preprints.org) | NOT PEER-REVIEWED | Posted: 3 November 2023 doi:10.20944/preprints202311.0203.v1

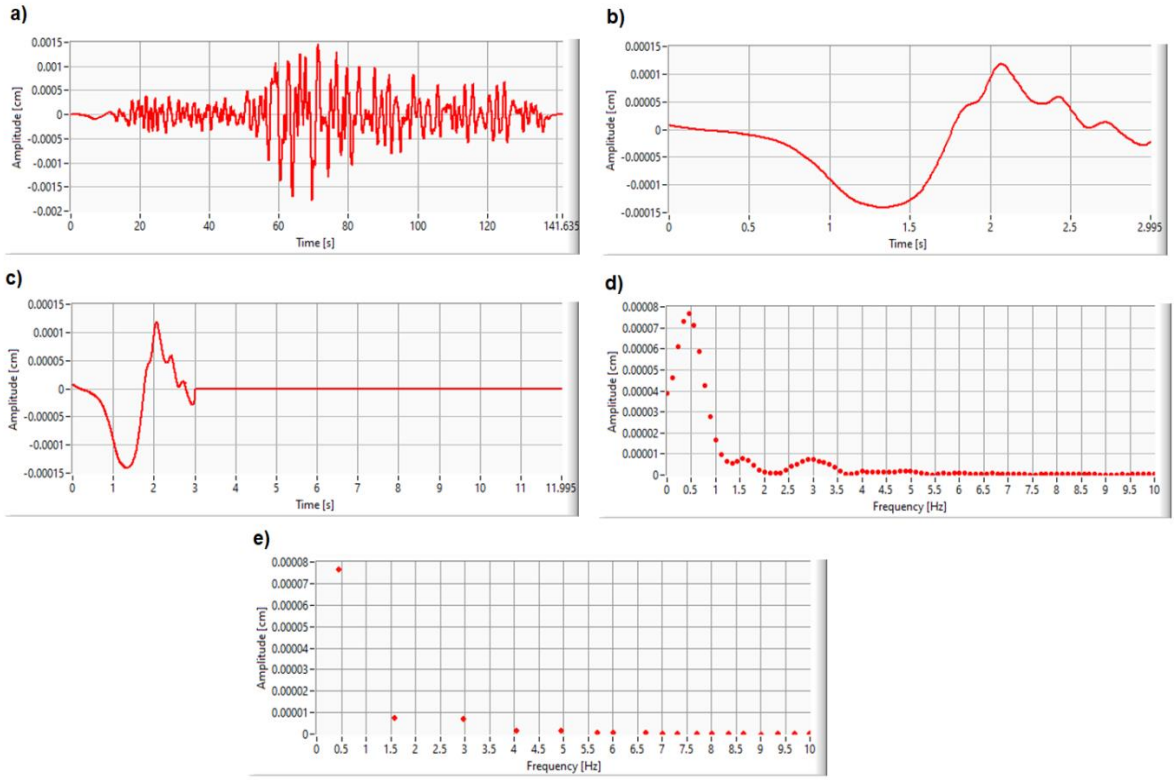

Figure 1. Attainment of the characteristic period of the seismic P wave estimation in the frequency domain.

3. Results

Herein was developed a method for calculating the characteristic period of the P wave of earthquakes based on the frequency spectrum of the displacement wave. Three types of validation tests were carried out, one with signals containing a single spectral component (a pure sinusoidal signal), one with signals with two spectral components and one with three spectral components, having different values of frequencies and amplitudes.

Testing with a signal having single spectral component (Figure 2). A set of sinusoidal signals of 3 units amplitude was used, for which the frequency was varied between 0.3 Hz and 20 Hz, the range covering the area of interest for EEW systems. The variation step was 0.1 Hz. For each signal, the characteristic frequency and the characteristic period were calculated by the three methods (the time-domain classic method M1, the frequency-domain method M2 and the proposed method M3) and the absolute errors compared to the reference were determined. The column of graphs on the left in Fig. 2 shows the absolute errors for the characteristic frequency and the column on the right for the characteristic period, for the three methods M1, M2 and M3.

Preprints (www.preprints.org) | NOT PEER-REVIEWED | Posted: 3 November 2023 doi:10.20944/preprints202311.0203.v1

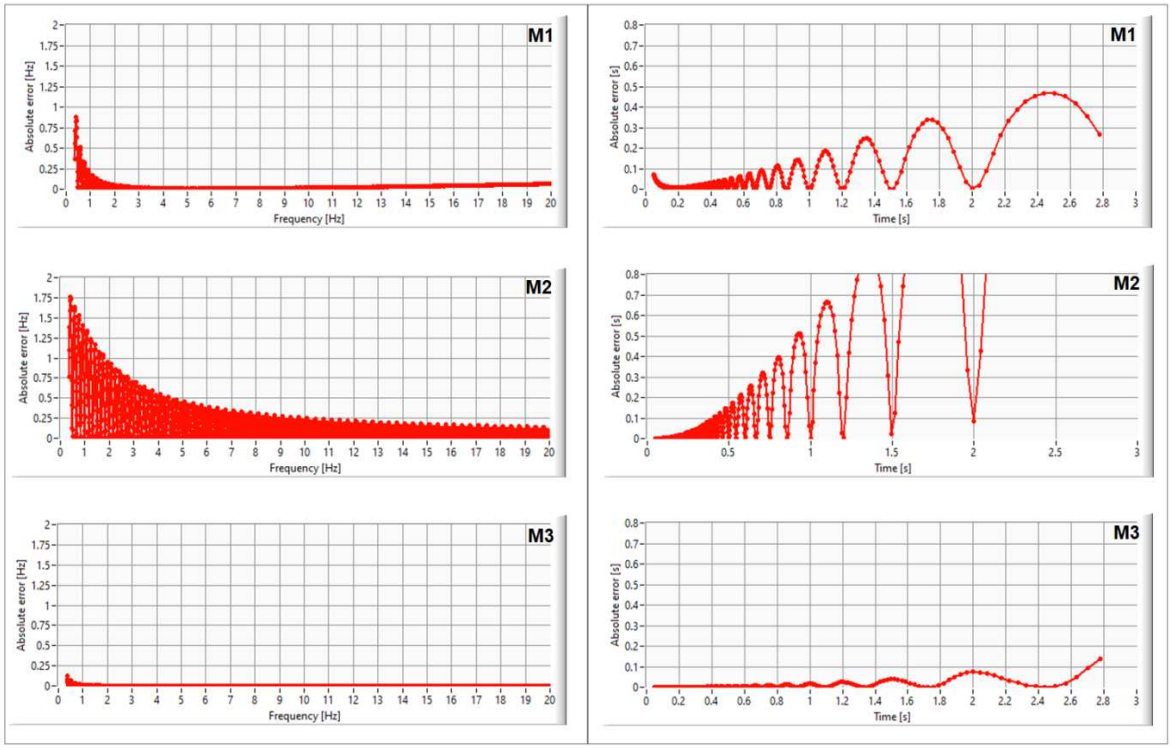

Figure 2. The absolute error graph of the three compared methods, in frequency-domain (left) and time-domain (right) calculation, for singular spectrum signal.

It can be observed that for all methods the errors increase with the decrease of the frequency and implicitly with the increase of the period. The M2 method presents almost double absolute errors compared to the classical method M1, while the proposed method M3 presents errors reduced to at least one third compared to the classical method.

Testing with a signal having two spectral components (Fig. 3.a). There was used a set of synthetic signals from a sinusoidal signal of 8 units amplitude and 0.9 Hz frequency and a sinusoidal signal of 3 units amplitude, for which the frequency was varied between 0.3 Hz and 20 Hz. For each signal, the characteristic frequency and the characteristic period were determined by the three methods, then were calculated the absolute errors compared to the reference (parameters imposed on the signal synthesis) and plotted in Fig. 3.a. It can be observed within this test as well, for all methods, the errors increase with decreasing frequency and increasing period. The M2 method presents almost double errors compared to the classical method M1, while the proposed method M3 presents errors reduced to at least one third compared to the classical method.

Testing with a signal having three spectral components (Fig. 3.b). There was used a set of synthetic signals from a sinusoidal signal of 8 units amplitude and 0.9 Hz frequency, a sinusoidal signal of 2.7 units amplitude and 1.3 Hz frequency and a sinusoidal signal of 3 units amplitude, for which the frequency was varied between 0.3 Hz and 20 Hz. Similarly, the frequencies and characteristic periods were calculated by the three methods. Comparing the absolute errors from Fig.3.a with Fig.3.b in the corresponding domain, it is found that there is no change in the ratio between the errors of the three methods with the increase in the number of harmonics. This fact asserts the proposed method leads to a reduced standard deviation compared to the classical method, also for multicomponent waveforms.

Preprints (www.preprints.org) | NOT PEER-REVIEWED | Posted: 3 November 2023 doi:10.20944/preprints202311.0203.v1

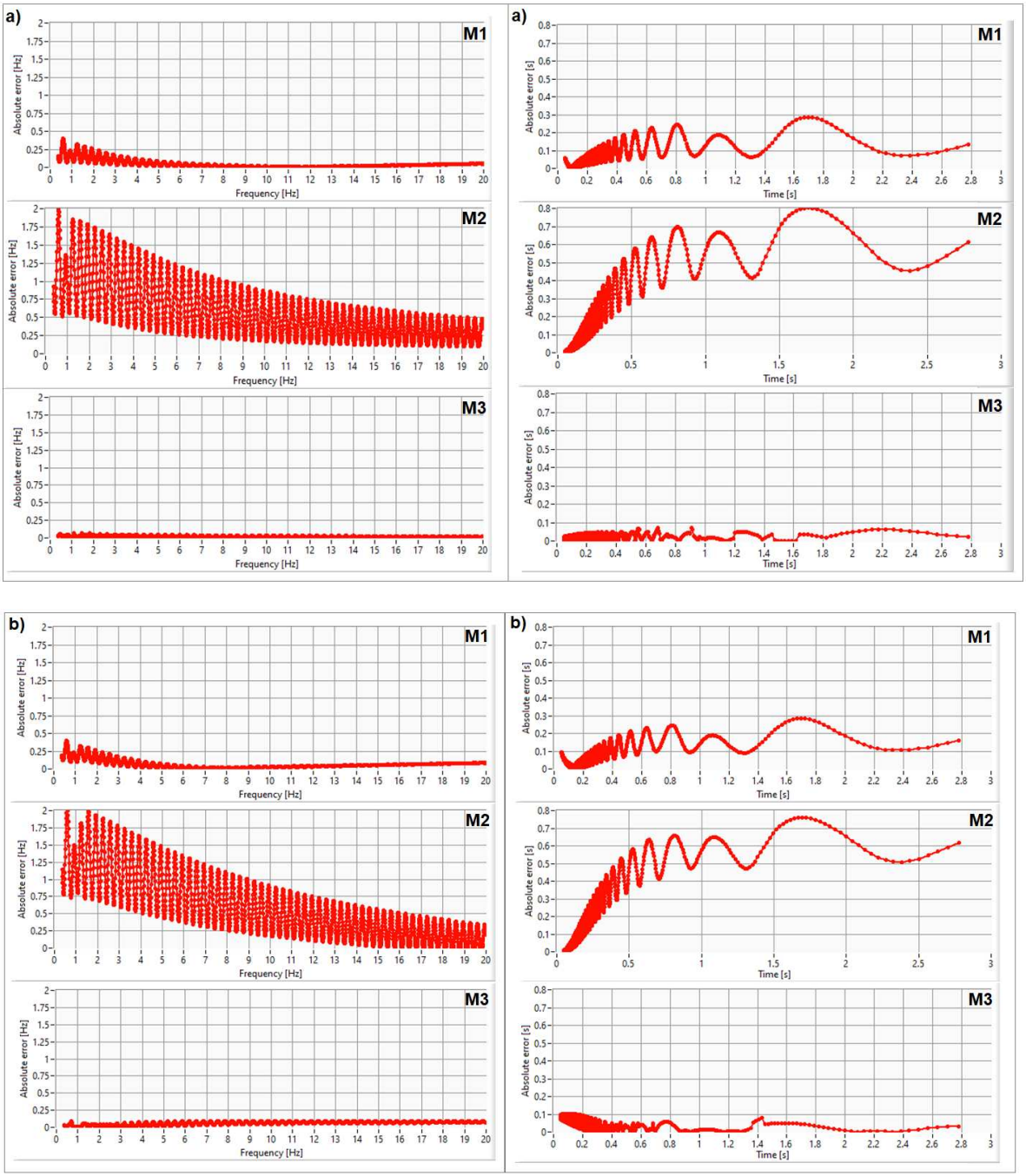

Figure 3. The absolute error graph of the three compared methods, in frequency-domain (left) and time-domain (right) calculation, for multicomponent signal – two spectra (a), three spectra (b).

Standard deviation evaluation. A comparison was made between the classical method and the proposed method, subjected to the dispersion of the values of the characteristic period of an earthquake, when several stations that simultaneously record an event are taken into account. Thus, for a given earthquake, characterized by the seismic waves recorded at N different stations, the average value of the characteristic period and the standard deviation were calculated. This reasoning was applied on the vertical waves of 3 earthquakes occurred 2023, having the main parameters render in Table 1, whose records at 200 Hz were taken from the (ESM Database [31]).

Preprints (www.preprints.org) | NOT PEER-REVIEWED | Posted: 3 November 2023 doi:10.20944/preprints202311.0203.v1

Table 1. Standard deviation of the seismic characteristic period calculated with time-domain method (M1) and proposed method (M3).

Event /Date	Magnitude [Mw]	Dmax [km]	No. of stations (N)	Classic method (M1)		Proposed method (M3)	
				Mean [s] $\bar{\tau_c}$	Standard deviation [s] $s(\tau_c)$	Mean [s] $\bar{\tau_c}$	Standard deviation [s] $s(\tau_c)$
20230621_0000149/ 21.06.2023	4.1	113	7	0.31	±0.13	0.28	±0.11
20230606_0000145/ 06.06.2023	4.7	293	13	0.63	±0.28	0.52	±0.15
20230214_0000139/ 14.02.2023	5.5	269	24	0.98	±0.31	1.11	±0.22

D_{max} represents the distance between the epicenter and the farthest station from which the recording of the considered earthquake was used. N is the number of stations from which records of a certain earthquake were taken. The average characteristic period was calculated with:

$$\bar{\tau_c} = \frac{\sum_1^N \tau_{c_i}}{N}$$

And the standard deviation with:

$$s(\tau_c) = \frac{\sum_1^N (\bar{\tau_c} - \tau_{c_i})^2}{N-1}$$

Results from the Table 1 turn out that using the proposed method (M3) leads to a smaller dispersion for each earthquake, compared to the classic method (M1).

4. Discussion

Testing the proposed method, to determine the characteristic period by calculating the characteristic frequency from the frequency spectrum of the signal, was carried out in two ways: by simulation and by calculation on real P-wave signals obtained from earthquake recordings.

Testing the Method by Simulation

Synthesized signals with precisely known frequency/period were used for testing. For these signals, the frequency/period was calculated using:

- the classical method M1 from the time domain, that uses the ratio between speed and displacement,
- the method M2 based on eq. (4) - which derives directly from the classical method, by correspondence in frequency,
- the proposed method M3.

Method M1 provides results in time and M2 and M3 provide results in frequency. In order to make comparisons from the point of view of absolute errors both as characteristic period and as characteristic frequency, the characteristic period obtained by M1 was converted into characteristic frequency and the characteristic frequencies obtained by M2 and M3 into characteristic periods.

Tests were carried out with pure sinusoidal signals and with sinusoidal signals with harmonics and the graphs of the absolute errors obtained for the three methods were plotted. The following are observed:

- • switching to the frequency domain (M2) does not provide better results compared to the classical method;
- • the application of the M3 method leads to the reduction of relative errors for all test variants with synthesized signals regardless of the number of harmonics or the frequency values of the harmonics.
- • because P wave sequences are limited to 3 seconds, signals with frequencies below 0.3Hz or periods of more than 3s will contain less than one period of the useful signal.

 doi:10.20944/preprints202311.0203.v1

Thus, for all methods, the errors increase at low frequencies and implicitly at long periods and represent the area where saturation occurs for large earthquakes.

Testing the Method with Real P Waves

Since the work refers to a method of estimating the characteristic period of the P wave of earthquakes, the testing with real P waves was carried out only from the point of view of estimating the period and validating the simulation testing. Forecasting the magnitude based on the P wave is dependent on the soil structure in the direction of earthquake propagation, from the epicenter to the seismic station where the wave is recorded, being a geophysical dependence. For the test, 44 seismic recordings from different stations were used, recordings belonging to three earthquakes. For each recording, the characteristic period was determined by M1 and M3. The periods were grouped by the three earthquake events and the average value and standard deviation were calculated for each. Analyzing the obtained data, it can be seen that the proposed method leads to smaller standard deviations than those obtained by the classical method. Also, the average of the period obtained by M1 falls within the range of variation of the average obtained before M3 for all three earthquakes, as well as the average of the period obtained by M3 also falls within the range of variation of the average obtained by M1.

5. Conclusions

Most earthquake early warning systems use to predict the event magnitude and the peak ground acceleration parameters attained from the initial P waves, recorded at close seismic stations. Commonly the peak amplitudes of displacement, along with the characteristic period and the integral of squared velocity are used to compute through specific algorithms the level of the danger and the necessity for EEWS to trigger the emergency alarm. Estimating the characteristic period τ_c involves inputs as velocity and acceleration from multiple P-waves similarly recorded in several seismic stations. As τ_c ascends with earthquake's magnitude and it's independent on the distance between the earthquake epicenter and an observation station up to a few hundred kilometers away, settle that it's a key factor in EWS regional seismic prediction.

The proposed method, for calculating the characteristic period of the seismic P wave in the frequency domain, has a lower standard deviation than the classical method. Tests carried out through synthetic signals, with a single tone or with harmonic content, reveal that the determination errors of the characteristic period are smaller when using this method. Statistical tests to evaluate the standard deviation in which earthquake records from several stations were interpreted also revealed a superior behavior of the proposed method. In this context we consider that this method can be used with good results in magnitude prediction applications based on the characteristic period of the initial wave.

Author Contributions: C.D. - conceptualization and research; C.D. and M.C.T. - validation, formal analysis and data curation; C.D. and E.S. – data usage, visualization and writing the manuscript. All authors have read and agreed to the published version of the manuscript.

Funding: This research was funded by European Regional Development Fund, grant number 7227/19.11.2021 (SMIS code 137414) — "Seismic warning system with automatic unlocking of entrance doors with interphone". The APC was funded by "Gheorghe Asachi" Technical University of Iași, România.

Data Availability Statement: Not applicable here.

Conflicts of Interest: The authors declare no conflict of interest. The funders had no role in the design of the study; in the collection, analyses, or interpretation of data; in the writing of the manuscript; or in the decision to publish the results.

References

1. Posadas, A.; Pasten, D.; Vogel, E. E.; Saravia, G. Earthquake hazard characterization by using entropy: application to northern Chilean earthquakes. *Nat. Hazards Earth Syst. Sci*. **2023**, *23(5)*, 1911-1920.

2. Pasten, D.; Vogel, E.E.; Saravia, G.; Posadas, A.; Sotolongo, O. Tsallis Entropy and Mutability to Characterize Seismic Sequences: The Case of 2007–2014 Northern Chile Earthquakes. *Entropy* **2023**, *25*, 1417.
3. Ohsawa, Y. Regional Seismic Information Entropy to Detect Earthquake Activation Precursors. *Entropy* **2018**, *20*, 861.
4. Posadas, A.; Morales, J.; Ibañez, J. M.; Posadas-Garzon, A. Shaking earth: Non-linear seismic processes and the second law of thermodynamics: A case study from Canterbury (New Zealand) earthquakes. *Chaos, Solitons & Fractals* **2021**, *151*, 111243.
5. Zaccagnino, D.; Telesca, L.; Doglioni, C. Different Fault Response to Stress during the Seismic Cycle. *Appl. Sci.* **2021**, *11*, 9596.
6. McGuire, J. J. Seismic cycles and earthquake predictability on East Pacific Rise transform faults. *Bull. Seismol. Soc. Am.* **2008**, *98(3)*, 1067-1084.
7. Ide, S. Frequent observations of identical onsets of large and small earthquakes. *Nature* **2019**, *573 (7772)*, 112-116.
8. Meier, M.A.; Kodera, Y.; Böse, M.; Chung, A.; Hoshiba, M.; Cochran, E. How often can Earthquake Early Warning systems alert sites with high-intensity ground motion?. *J. Geophys. Res. Solid Earth* **2020**, *125(2)*, e2019JB017718.
9. Okuda, T.; Ide, S. Hierarchical rupture growth evidenced by the initial seismic waveforms. *Nature Comm.* **2018**, *9(1)*.
10. Meier, M.-A.; Heaton, T.; Clinton, J. Evidence for universal earthquake rupture initiation behavior. Geophys. Res. Lett. **2016**, *43(15)*, 7991–7996.
11. Nakamura, Y.; Tucker, B.E. Japan's Earthquake Warning System: Should it be Imported to California?. *Calif. Geology* **1988**, *41 (2)*, 33-40.
12. Nakamura, Y.; Saita, J. UrEDAS, the Earthquake Warning System: Today and Tomorrow. In *Earthquake Early Warning* Systems; Gasparini, P., Manfredi, G., Zschau, J., Eds.; Publisher: Springer, Berlin Heidelberg, 2007; pp. 249-281.
13. Wang, Y.; Li, S.; Song, J. Threshold-based evolutionary magnitude estimation for an earthquake early warning system in the Sichuan–Yunnan region, China. *Sci Rep* **2020**, *10*, 21055.
14. Cremen, G.; Galasso, C.; Zuccolo, E. Investigating the potential effectiveness of earthquake early warning across Europe. *Nat Commun* **2022**, *13*, 639.
15. Lior, I., Rivet, D., Ampuero, JP. *et al*. Magnitude estimation and ground motion prediction to harness fiber optic distributed acoustic sensing for earthquake early warning. *Sci Rep* **2023**, *13*, 424.
16. Furuya, I. Predominant Period and Magnitude. *J. Phys. Earth.* **1969**, *17 (2)*, 119-126.
17. Kanai, K. On the Predominant Period of Earthquake Motions. *Bull. Earthq. Res. Inst. Univ. Tokyo* **1961,** *40*, 855-860.
18. Nakamura, Y. On the Urgent Earthquake Detection and Alarm System (UrEDAS). In Proceedings of the 9th World Conference on Earthquake Engineering, vol. 7, 673–678 (1988).
19. Allen, R.M., Kanamori, H. The Potential for Earthquake Early Warning in Southern California. *Science* **2003**, *300*, 786–789.
20. Kanamori, H. Real-Time seismology and earthquake damage mitigation. *Annu. Rev. Earth Planet. Sci.* **2005**, *33*, 195–214.
21. Cheng Z.; Peng C.; Chen M. Real-Time Seismic Intensity Measurements Prediction for Earthquake Early Warning: A Systematic Literature Review. *Sensors* **2023**, *23 (11)*, 5052.
22. Yusof, K.A.; Abdullah, M.; Hamid, N.S.A.; Ahadi, S.; Yoshikawa, A. Correlations between Earthquake Properties and Characteristics of Possible ULF Geomagnetic Precursor over Multiple Earthquakes. *Universe* **2021**, *7*, 20.
23. Hsu, T.Y.; Wu, R.T.; Liang, C.W.; Kuo, C.H.; Lin, C.M. Peak ground acceleration estimation using P-wave parameters and horizontal-to-vertical spectral ratios. *Terr. Atmos. Ocean. Sci.* **2020**, *31*, 1-8.
24. Zlydenko, O.; Elidan, G.; Hassidim, A. A neural encoder for earthquake rate forecasting. *Sci Rep* **2023**, *13*, 12350.
25. Abdalzaher, M.S.; Krichen, M.; Yiltas-Kaplan, D.; Ben Dhaou, I.; Adoni, W.Y.H. Early Detection of Earthquakes Using IoT and Cloud Infrastructure: A Survey. *Sustainability* **2023**, *15*, 11713.
26. Xue, K.; Zhang, W.; Wang, Z.; Jin, Y.; Guo, X.; Chen, Y. Real Aperture Continuous Terahertz Imaging System and Spectral Refinement Method. *Photonics* **2023**, *10*, 1020.
27. Zhou, P.; Shi, T.; Xin, J.; Li, Y.; Lv, T.; Zang, L. Extended Smoothing Methods for Sparse Test Data Based on Zero-Padding. *Appl. Sci.* **2023**, *13*, 4816.
28. Naghizadeh, M.; Innanen, K.A. Two-dimensional fast generalized Fourier interpolation of seismic records. *Geophys. Prospect*. **2013**, *61*, 62-76.

29. Van Dinh, N.; Basu, B. Zero-pad effects on conditional simulation and application of spatially-varying earthquake motions. 6th European Workshop on Structural Health Monitoring - Tu.3.D.3, Dresden, Germany, 3-6 July 2012.
30. Chen, Y.; He, Y.; Li, S.; Wu, H.; Peng, Z. Seismic spectrum decomposition based on sparse time-frequency analysis. *J Appl Geophy* **2020**, *177*, 104031.
31. Luzi L.; Lanzano G.; Felicetta C.; D'Amico M. C.; Russo E., *et.al*. Engineering Strong Motion Database (ESM) (Version 2.0). Istituto Nazionale di Geofisica e Vulcanologia (2020). https://esm-db.eu/#/event/search